ARCHIVES OF CIVIL AND MECHANICAL ENGINEERING

Vol. X 2010 No. 2

Experimental study on ultimate strength of CK20 steel cylindrical panels subjected to compressive axial load

M. SHARIATI, M. SEDIGHI, J. SAEMI, H.R. EIPAKCHI, H.R. ALLAHBAKHSH
Mechanical Engineering Faculty, Shahrood University of Technology, Shahrood, P.O. Box 316, I.R., Iran.

In this paper, the effects of the length, sector angle and boundary conditions on the buckling load and post-buckling behaviour of cylindrical panels have been studied, experimentally. The compressive axial load has been applied on the panels using servo-hydraulic machine and different boundary conditions have been prepared by suitable fixtures. The presented results can be used in designing of these structures.

Keywords: *buckling, post-buckling, cylindrical panels, experimental test*

1. Introduction

The shell structures are important in various engineering fields. The buckling load, is usually the most criterion in designing of a long thin shell. The classification and design codes for aircraft, space vehicles, ships, offshore platforms, trains and cold formed sections are all based mostly on experimental findings and semi empirical formulas. Based on the classic theories, the buckling load of thin cylindrical shells subject to uniform axial compression can be predicted using the formula:

$$N_{cr} = \frac{E}{\sqrt{3(1-\nu^2)}}\left(\frac{t^2}{R}\right). \tag{1}$$

where:

E is the Young's modulus,
ν is Poisson's ratio,
t is shell thickness,
R is shell radius.

It is noteworthy that this formula gives an appropriate result for thin shells without cutouts with $L/R \leq 5$ [1]. For shells with moderate thickness ($R/t < 50$), this formula often overestimates the buckling load, so that buckling occurs before reaching the specified load. An analytical solution for the buckling load of isotropic and orthotropic panels has been presented by Timoshenko [2] and Lekhnitskii [3]. Magnucki [4] solved the Donnell's equation for buckling of panels with three edges simply supported and one

edge free subjected to axial load using the Galerkin method. Patel [5] discussed on static and dynamic stability of panels with the edge harmonic loading. Jiang [6] studied the buckling of panels subjected to compressive stress using the differential quadrature element method. The most experimental works, relates to the buckling of columns and cylinders. Young [7] presented an experimental investigation of concrete-filled cold-formed high strength stainless steel tube columns subjected to uniform axial compression. He studied the effects of the tube shape, plate thickness and concrete strength. The test results were compared with American and Australian standards. Zhu [8–9] studied experimentally the failure modes and strengths of aluminium alloy with and without transverse weld subjected to pure axial compression between fixed ends. The observed failure modes include yielding and buckling for different lengths. The test results were compared with some standards for aluminium structures. Liu [10] described a test procedure on cold-formed stainless steel square hollow sections subjected to pure axial compression. He concluded that design rules in Australian standard are slightly more reliable than the design rules in the American and European specifications for performed tests. Zhang [11] presented experimental and numerical investigations on the performance of repaired thin-skinned, blade-stiffened composite panels in the post-buckling range. The results showed that under the present repair scheme, the strength of the panel can be recovered satisfactorily. Further, the repair scheme was seen capable of restoring the general load path in the panels as well as the general post-buckling behaviour. Lanzi [12] reported the results of an experimental investigation on stringer-stiffened panels made of carbon fabric reinforced plastic. The axial compression tests were performed up to collapse. Experimental data demonstrated the strength capabilities of the identified structures to operate in post buckling, allowing further weight savings.

In this paper, the effects of the length, sector angle and different boundary conditions on instability of steel cylindrical panels have been studied experimentally. Also, the behaviour of the panels in post-buckling path has been shown.

2. Theoretical analysis: buckling of circular cylindrical panels under axial compression

Consider a simply supported, cylindrical panel of length L, radius R, thickness t and central angle φ. The panel is under a uniform axial compressive force N as shown in Figure 1.

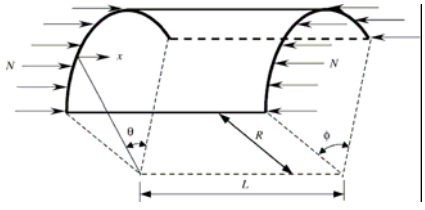

Fig. 1. Cylindrical panel under compression

For the buckling of cylindrical shells, the governing differential equations are given by

$$\frac{\partial^2 u}{\partial x^2}+\frac{1+\nu}{2R}\frac{\partial^2 v}{\partial x\partial\theta}-\frac{\nu}{R}\frac{\partial w}{\partial x}+\frac{1-\nu}{2R^2}\frac{\partial^2 u}{\partial\theta^2}=0, \tag{2}$$

$$\begin{aligned}&\frac{1+\nu}{2R}\frac{\partial^2 u}{\partial x\partial\theta}+\frac{1-\nu}{2}\frac{\partial^2 v}{\partial x^2}+\frac{1}{R^2}\frac{\partial^2 v}{\partial\theta^2}-\frac{1}{R^2}\frac{\partial w}{\partial\theta}-\frac{N(1-\nu^2)}{Et}\frac{\partial^2 v}{\partial x^2}\\&\quad+\frac{t^2}{12R^2}\left[\frac{1}{R^2}\frac{\partial^2 v}{\partial\theta^2}+\frac{1}{R^3}\frac{\partial^3 w}{\partial\theta^3}+\frac{\partial^3 w}{\partial x^2\partial\theta}+(1-\nu)\frac{\partial^2 v}{\partial x^2}\right]=0,\end{aligned} \tag{3}$$

$$\begin{aligned}&\nu\frac{\partial u}{\partial x}+\frac{1}{R}\frac{\partial v}{\partial\theta}-\frac{w}{R}-\frac{t^2}{12R^2}\\&\left[\frac{1}{R}\frac{\partial^3 v}{\partial\theta^3}+(2-\nu)R\frac{\partial^3 w}{\partial x^2\partial\theta}+R^3\frac{\partial^4 w}{\partial x^4}+\frac{1}{R}\frac{\partial^4 w}{\partial\theta^4}+2R\frac{\partial^4 w}{\partial x^2\partial\theta^2}\right]-\frac{NR(1-\nu^2)}{Et}\frac{\partial^2 w}{\partial x^2}=0,\end{aligned} \tag{4}$$

in which u, v, w are the longitudinal displacement, tangential displacement and radial displacement, respectively. The displacement functions are, however, given by

$$u=\sum_m^\infty\sum_n^\infty A_{mn}\sin\frac{n\pi\theta}{\phi}\cos\frac{m\pi x}{L}, \tag{5}$$

$$v=\sum_m^\infty\sum_n^\infty B_{mn}\cos\frac{n\pi\theta}{\phi}\sin\frac{m\pi x}{L}, \tag{6}$$

$$w=\sum_m^\infty\sum_n^\infty C_{mn}\sin\frac{n\pi\theta}{\phi}\sin\frac{m\pi x}{L}. \tag{7}$$

where:

A_{mn}, B_{mn}, C_{mn} are the unknown buckling amplitudes. By substituting Equations (5) to (7) into Equations (2) to (4), we obtain

$$N=\frac{Et}{(1-\nu^2)}\left[\frac{t^2}{12R^2}\frac{\left(\frac{n^2\pi^2}{\phi^2}+\beta^2\right)^2}{\beta^2}+\frac{(1-\nu^2)\beta^2}{\left(\frac{n^2\pi^2}{\phi^2}+\beta^2\right)^2}\right]. \tag{8}$$

Denoting $\beta = \dfrac{m\pi R}{L}$. Therefore, the buckling load for a cylindrical panel under uniform axial compression is given by

$$N_{\min} = \frac{1}{\sqrt{3(1-\nu^2)}}\left(\frac{Et^2}{R}\right). \tag{9}$$

When the angle φ is very small, the buckling behaviour of the cylindrical panel approaches that of a longitudinally compressed rectangular plate.

3. Experimental study

Some specimens with different lengths and sector angles have been prepared. All the specimens have been manufactured from one tube branch and so, they have the same radius and thickness. Figure 2 shows schematic of a panel and the dimensions have been listed in Table 1. The bucking tests were performed using a servo-hydraulic machine (INSTRON 8802). This universal test machine includes a hydraulic actuator for applying axial load on panels and two load cells with capacities 25 kN and 250 kN for different applications. The test results can be transmitted to a computer.

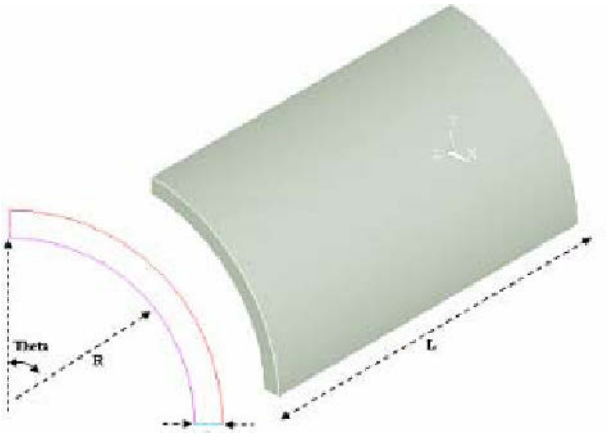

Fig. 2. Schematic of panels

Table 1. Geometrical and mechanical properties of panels

D = 42 mm	Diameter
t = 2 mm	Thickness
Θ = 90°, 120°, 180°, 355°, Complete	Sector angle
L = 100, 150, 250 mm	Length
σ_y = 340 MPa	Yield stress
E = 192 GPa	Elasticity modulus

3.1. Mechanical properties

The mechanical properties of the metal panels have obtained using the tensile test. The dimensions of tensile test specimens which are cut from the original tube, have been chosen according to

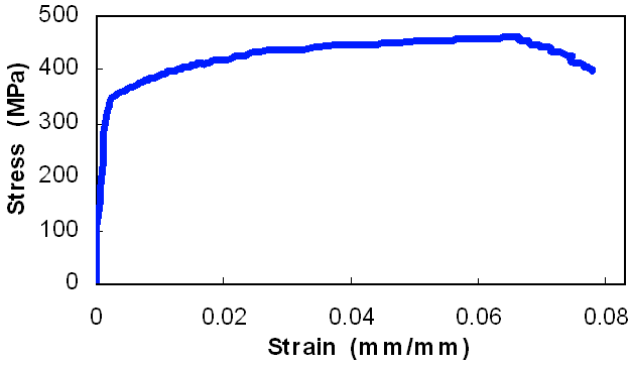

Fig. 3. Stress-strain diagram

ASTM E8 standard [13]. Figure 3 shows the stress-strain diagram for this material. The Young's modulus and the yield stress which are listed in Table 1 have been determined from Figure 3.

3.2. Boundary conditions

Two types of fixtures were designed to simulate the simply supported and clamped boundary conditions for the arc ends. Figure (4a) shows a fixture for simply supported conditions. It does not have any resistance to rotation. A fixture for clamped boundary conditions has been shown in Figure (4b). It has a narrow width and a deep slot, so the zero slope condition at the end, is reasonable.

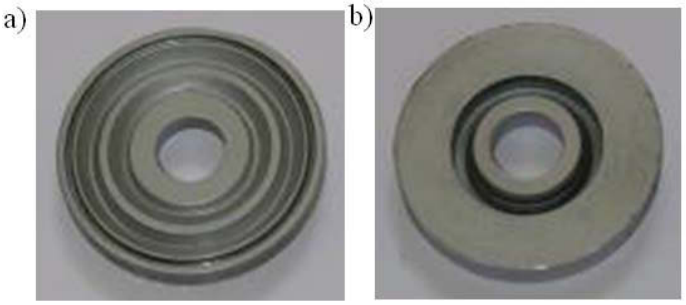

Fig. 4. a) Simply supported fixture, b) Clamped supported fixture

4. Buckling test

For the buckling test, an axial load was applied on the panels and by measuring the axial displacement, the load-displacement diagram was determined. These tests were performed for different panels with clamped and simply supported boundary condition. In all tests (except for a complete cylinder), the straight edges are free and the simple or clamped supports were applied on arc edges of panels. Figure 5 shows the test setup.

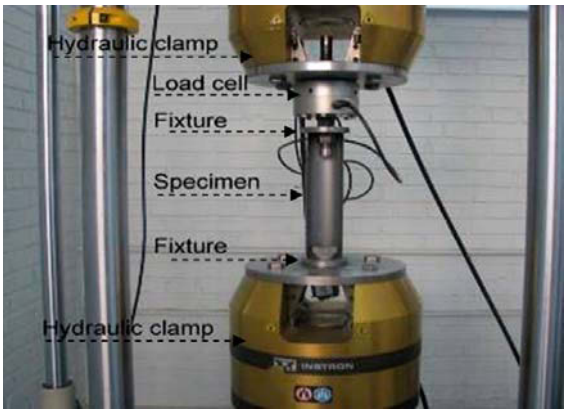

Fig. 5. Experimental test setup

4.1. Length effect

For investigation of the length effect, the buckling test was performed on some panels with the same angle and different lengths. The load-displacement for each panel was drawn. The peak values stand for the ultimate strength. For example, Figure 6 is the load – displacement diagrams for different lengths with $\theta = 90°$.

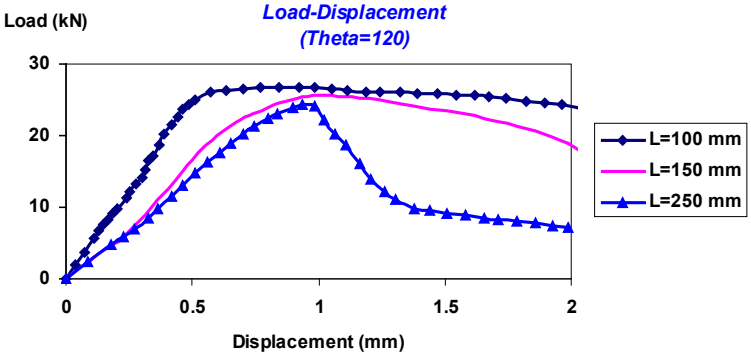

Fig. 6. Load-displacement diagram ($\theta = 120°$, simple supports)

Figure 7 shows the variation of the buckling load in terms of the length for different sector angles. The "Perfect" in Figure 7 stands for a cylinder ($\theta = 360°$). Deformations of tested panels have been shown in Figure 8. The experimental tests show that by decreasing the panel length, the buckling load will increase slightly.

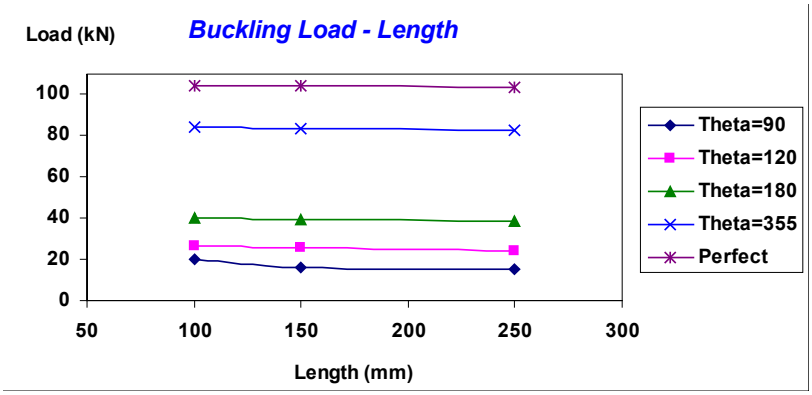

Fig. 7. Buckling load in terms of the length (for different sector angles)

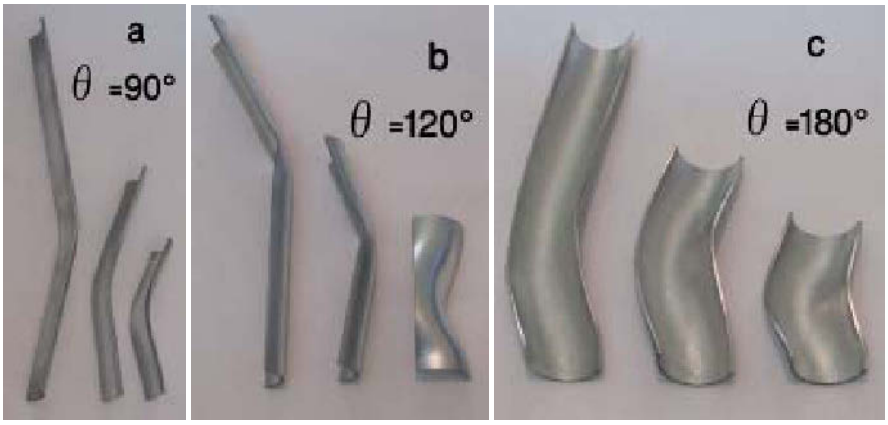

Fig. 8. Buckling mode shapes of panels with the same sector angles and different lengths (L = 100, 150, 250 mm), a) $\theta = 90°$, b) $\theta = 120°$, c) $\theta = 180°$

4.2. Sector angle effect

Some experimental tests were performed on panels with L = 100 mm and $\theta = 90°$, 120°, 180°, 355°, 360°. In Figure 9, the load-displacement diagrams for panels with different sector angle have been shown. $\theta = 355°$ corresponds to a narrow cutting on the original tube as Figure 10. Figure 11 shows the variations of the buckling load in terms of θ for different lengths and Figure 12 shows the buckling stress which it has been defined easily as the ratio of the load to cross section.

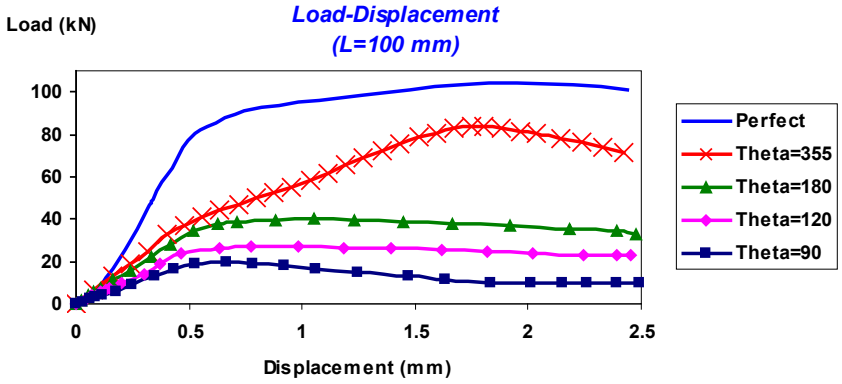

Fig. 9. Load-displacement diagram (L = 100 mm, simple supports)

Fig. 10. Panel deformation (L = 100 mm, θ = 355°)

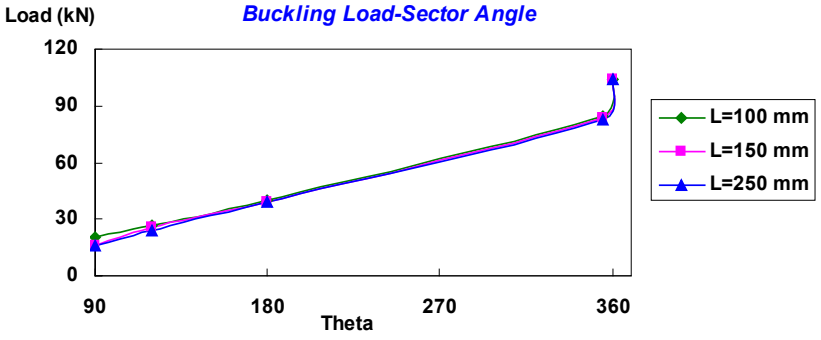

Fig. 11. Variations of buckling load in terms of sector angle for different lengths (simple supports)

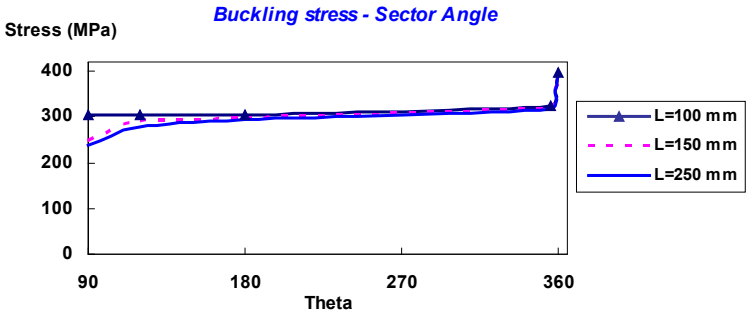

Fig. 12. Variations of buckling stress in terms of sector angle for different lengths (simple supports)

4.3. Boundary conditions effect

By changing the boundary conditions from simple to clamped, the degrees of freedom of supports reduce and the buckling load will increase. Figures 13–15 show the load-displacement diagrams for panels (θ = 90°) with different boundary conditions and the buckling loads have been listed in Table 2.

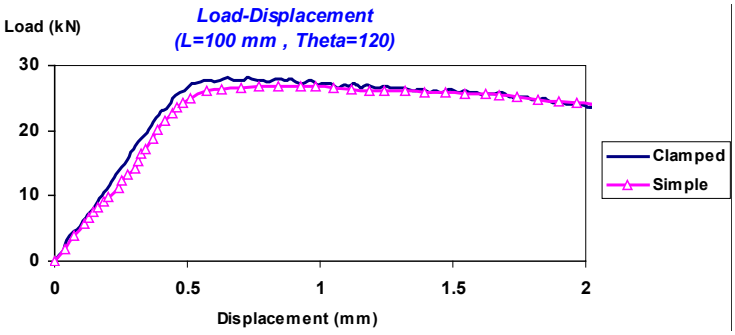

Fig. 13. Load-displacement diagram for clamped and simple supports (L = 100 mm, θ = 120°)

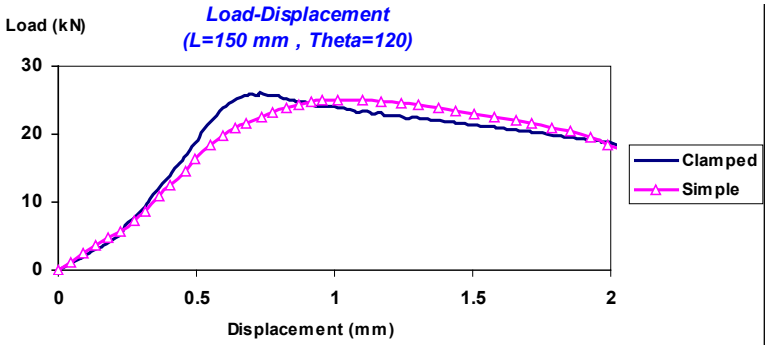

Fig. 14. Load-displacement diagram for clamped and simple supports (L = 150 mm, θ = 120°)

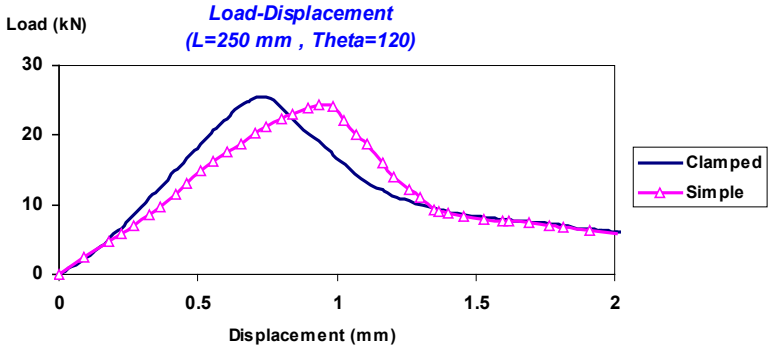

Fig. 15. Load-displacement diagram for clamped and simple supports (L = 250 mm, θ = 120°)

Table 2. Buckling loads (kN) for panels with clamped and simple supports

	θ = 90°		θ = 120°		θ = 180°		θ = 355°		θ = 360°	
	Simple	Clamped	Simple	Clamped	Simple	Clamped	Simple	Clamped	Simple	Clamped
L = 100 (mm)	19.85	20.05	26.75	28.18	39.50	39.86	84.09	85.62	106.91	–
L = 150 (mm)	15.98	16.37	25.11	26.04	38.81	39.21	83.39	85.27	105.26	–
L = 250 (mm)	14.95	15.64	24.33	25.58	38.05	38.87	82.89	84.13	103.73	104.48

4.4. Effect of eccentric loading

In this section, the effect of eccentric loading on the buckling behaviour of cylindrical panel under combined loading is studied by emphasizing on panel with similar length and three sector angle of 90°, 120° and 180°.The results indicate that buckling load is more sensitivity to eccentric load and only the eccentricity (X = 51 mm) for specimens (L = 100 mm), will cause the shell to buckle at 0.02 of axial compression load. Types of fixture were designed to simulate the combined loading and sensitivity of the cylindrical panel buckling to eccentricity is shown in Figure 16.

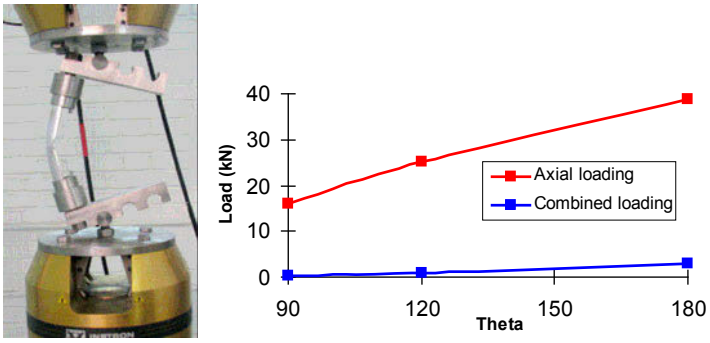

Fig. 16. Schematic of fixtures applying for combined loading and diagram of sensitivity of the panel buckling load to eccentricity

5. Confirmation of theoretical results with experimental findings

A curved plate loaded in axial compression buckle in the same manner as a cylinder when the plate curvature is large, and when the plate curvature is small it buckles essentially as a flat plate. Between these two limits there is a transition from one type of behaviour to the other. When load is applied to the plate it attains a critical load, after which the load suddenly drops. Upon further axial deformation the load continues to rise again and reaches a failure load which is greater than the buckling load if the latter occurs elastically. When the plate buckles plastically, buckling and failure are coincident.

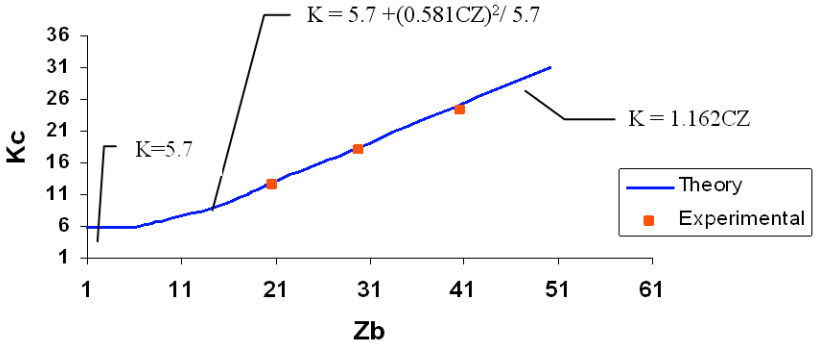

Fig. 17. Comparison of test data for (L = 150 mm, θ = 90°, 120°, 180°) with theory for axially compressed panels

Some of test data, for L = 150 mm in three different sector angle (θ = 90°, 120°, 180°), are shown in Figure 17 in terms of K_c and Z_b, where

$$Z_b = \left(1-v^2\right)^{0.5}\left(\frac{b^2}{rt}\right), \tag{10}$$

$$K_C = \frac{12\sigma_{cr}\left(1-v^2\right)}{\pi^2 E}\left(\frac{b}{t}\right)^2. \tag{11}$$

where:

E is the Young's modulus,
v is Poisson's ratio,
σ_{cr} is critical stress,
t is shell thickness,
r is shell radius,
b is width of cylindrical panel.

The boundary conditions of the panels tested were between simple supports and clamped. Thus an average of the buckling coefficients of these two limiting cases, K_{pl} = 5.7, was used for correlation purposes [14]. The theoretical results are in good agreement with the experimental tests.

6. Results

By increasing the length, the buckling load decreases slightly (Figure 7). This reduction is more for shorter lengths. Also by increasing the sector angle of a panel, the buckling load increases. It is possible to approximate the buckling load as

$$P = K\frac{\theta^n}{L^m}, \tag{12}$$

where k, m, n are constants and they depend on the geometrical and mechanical properties of panels.

In Figure 8, the deformed shape of the tested panels has been shown. For a short panel, it is snap-through like. For a long panel, it deforms like the Euler column and for a cylinder, it has a symmetric deformation. This symmetry can be approved the uniformity of the applied load. According to Figure 9, the existence of a narrow cutting (θ = 355°) can reduce the buckling load significantly. It may be due to reduction of the structure stiffness. Also the buckling load capacity of a complete cylinder is more than of this panel. Figure 10 shows the deformed shape of panel for this case. From Figures 11–12 the variations of the buckling load with respect to the sector angle is nearly linear expect for a cylinder. The yielding occurs before buckling in cylinder with L = 100 mm, so its results did not report in Figures 11–12. The buckling stress is constant approximately for θ > 90° or the buckling stress is not sensitive to the sector angle for tested specimens. For clamped boundary conditions, the buckling load is more than the simple support (Figures 13–15 Table 2). According to Figures 13–15 there is a delay of the buckling load by using simply supported boundary condition because the support permits the rotation in addition of axial displacement but in the clamped boundary conditions, there is no rotation or the structure is more restricted than the later case. In the other word, clamping the boundaries will increase the stiffness of the structure. The behaviour of the panel in post-buckling path may not be predicted or by changing the length (Figure 6), sector angle (Figure 9) and boundary conditions (Figures 13, 14); the behaviour of the panel will change. The results indicate that buckling load is more sensitivity to eccentric load (Figure 16). Figure 17 shows the theoretical results are in good agreement with the experimental tests. To check the repeatability of test, three tests have been performed for a panel with L = 150 mm, θ = 120°. The load-displacement diagrams have been shown in Figure 18 There is a good agreement between the results.

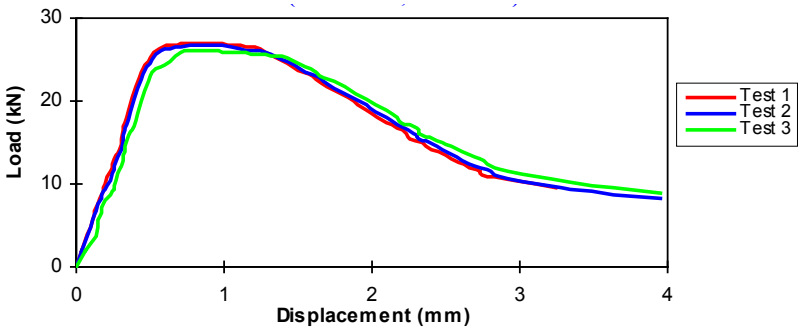

Fig. 18. Load-displacement diagram – test repeatability (L = 150 mm, θ = 120°)

7. Conclusions

The experimental tests show that:

1. By increasing the length of the panels, the bucking load decreases slightly. It is more important for short panels.
2. For $\theta > 90°$, by increasing the sector angle, the buckling load increases. Approximately, for tested panels, the buckling stress is not sensitive to the sector angle.
3. Clamped boundary conditions can increase the bucking load but the post-buckling path does not change significantly.
4. There is a delay of the buckling load by using simply supported boundary condition because, the simply support permits the rotation in addition of axial displacement but in the clamped boundary conditions structure is more restricted than the later case.
5. The existence of a longitudinal narrow slot will decrease the buckling load noticeably.
6. The results indicate that buckling load is more sensitivity to eccentric load.
7. The theoretical results are in good agreement with the experimental tests.

References

[1] Ugural A.C.: *Stresses in plates and shells*, New York, McGraw-Hill, 1981.
[2] Timoshenko S.P., Gere J.M.: *Theory of elastic stability*, New York, McGraw-Hill, 1961.
[3] Lekhnitskii S.G.: *Anisotropic plates*, Gordon and Breach, New York, 1968.
[4] Magnucki K., Mackiewicz M.: *Elastic buckling of an axially compressed cylindrical panel with three edges simply supported and one edge free*, Thin-Walled Structures, 2006, Vol. 44, No. 4, pp. 387–392.
[5] Patel S.N., Datta P.K., Sheikh A.H.: *Buckling and dynamic instability analysis of stiffened shell panels*, Thin-Walled Structures, 2006, Vol. 44, No. 3, pp. 321–333.
[6] Jiang L., Wang Y., Wang X.: *Buckling analysis of stiffened circular cylindrical panels using differential quadrature element method*, Thin-Walled Structures, 2008, Vol. 46, No. 3, pp. 390–398.

[7] Young B.: *Experimental and numerical investigation of high strength stainless steel structures*, Journal of Constructional Steel Research, 2008, Vol. 64, No. 11, pp. 1225–1230.
[8] Zhu J., Young B.: *Numerical investigation and design of aluminium alloy circular hollow section columns*, Thin-Walled Structures, 2008, Vol. 46, No. 12, pp. 1437–1449.
[9] Zhu J.H., Young B.: *Experimental investigation of aluminium alloy circular hollow section columns*, Engineering Structures, 2006, Vol. 28, No. 5, pp. 207–215.
[10] Liu Y., Young B.: *Buckling of stainless steel square hollow section compression members*, Journal of Constructional Steel Research, 2003, Vol. 59, No. 2, pp. 165–177.
[11] Zhang H., Motipalli J., Lam Y.C., Baker A.: *Experimental and finite element analyses on the post-buckling behaviour of repaired composite panels. Composites Part A*, 1998, Vol. 29, No. 11, pp. 1463–1471.
[12] Lanzi L.: *An experimental investigation on the post-buckling behaviour of composite stiffened panels*, 45th AIAA/ASME/ASCE/AHS/ASC Structures, Structural Dynamics & Materials Conference, California, 2004.
[13] ASTM A370-05, *Standard test methods and definitions for mechanical testing of steel products*.
[14] Gerard, George and Becker, Herbert: *Handbook of structural stability. Part 3: buckling of curved plates and shells*, NACA TN 3783, 1957.

Eksperymentalne badania wytrzymałości elementów cylindrycznych wykonanych ze stali CK20 poddanych osiowemu ściskaniu

W pracy przedstawiono eksperymentalne wyniki wpływu długości i kąta sektora próbek oraz warunków brzegowych na siłę wyboczenia oraz ich zachowanie się po wyboczeniu. Badania przeprowadzono na maszynie hydraulicznej, gdzie za pomocą odpowiednich uchwytów uzyskano różne warunki brzegowe. Przedstawione wyniki mogą być wykorzystane w projektowaniu struktur cylindrycznych.